Estimation of isotope variation of N_2O during denitrification by *Pseudomonas aureofaciens* and *Pseudomonas chlororaphis*: Implications for N_2O source apportionment

Joshua A Haslun[1, 3], Nathaniel E. Ostrom[2, 3], Eric L. Hegg[1, 3], Peggy H. Ostrom[2, 3]

[1]Biochemistry and Molecular Biology, Michigan State University, East Lansing, 48824, USA
[2]Integrative Biology, Michigan State University, East Lansing, 48824, USA
[3]Great Lakes Bioenergy Research Center, Michigan State University, East Lansing, 48824, USA

Correspondence to: Peggy H. Ostrom, Nathaniel E. Ostrom

Abstract. Soil microbial processes, stimulated by agricultural fertilization, account for 90 % of anthropogenic nitrous oxide (N_2O), the leading source of ozone depletion and a potent greenhouse gas. Efforts to reduce N_2O flux commonly focus on reducing fertilization rates. Management of microbial processes responsible for N_2O production may also be used to reduce N_2O emissions, but this requires knowledge of the prevailing process. To this end, stable isotopes of N_2O have been applied to differentiate N_2O produced by nitrification and denitrification. To better understand the factors contributing to isotopic variation during denitrification, we characterized the $\delta^{15}N$, $\delta^{18}O$ and site preference (SP; the intramolecular distribution of ^{15}N in N_2O) of N_2O produced during NO_3^- reduction by *Pseudomonas chlororaphis subsp. aureofaciens* and *P. c. subsp. chlororaphis*. The terminal product of denitrification for these two species is N_2O because they lack the gene nitrous oxide reductase, which is responsible for the reduction of N_2O to N_2. In addition to species, treatments included electron donor (citrate and succinate) and electron donor concentration (0.01 mM, 0.1 mM, 1 mM, and 10 mM) as factors. In contrast to the expectation of a Rayleigh model, all treatments exhibited curvilinear behaviour between $\delta^{15}N$ or $\delta^{18}O$ and the extent of the reaction. The curvilinear behaviour indicates that the fractionation factor changed over the course of the reaction, something that is not unexpected for a multi-step process such as denitrification. Using the derivative of the equation, we estimated that the net isotope effects (η) vary by as much as 100 ‰ over the course of a single reaction, placing challenges for using $\delta^{15}N$ and $\delta^{18}O$ as apportionment tools. In contrast, SP for denitrification was not affected by the extent of the reaction, the electron donor source, or concentration, although the mean SP of N_2O produced by each species differed. Therefore, SP remains a robust indicator of the origin of N_2O. To improve apportionment estimates with SP, future studies could evaluate other factors that contribute to the variation in SP.

1 Introduction

Agricultural production of food and energy has required a 10-fold increase (i.e. from 10 to 100 TGN yr^{-1}) in the application of synthetic fertilizer since 1950 (Robertson and Vitousek, 2009). Moreover, to maximize crop yields, nitrogen (N) is often applied at rates in excess of a crop's yield response, the average maximum crop yield as a function of fertilizer application rate. This results in a residual N pool (Sebilo et al., 2013). While some of the excess N may be incorporated into the soil, much of it is either transported out of the system via runoff as NO_2^- or NO_3^- (Zhou and Butterbach-Bahl, 2014), volatilized as NH_3 (Pan et al., 2016), or converted to N_2 and/or nitrous oxide (N_2O) via oxidative and reductive microbial processes (Schreiber et al., 2012; Venterea et al., 2012) such as nitrification, and denitrification, respectively. Stimulated by agricultural practices, these microbial processes account for 90 % of anthropogenic N_2O (Denman, 2007; Reay et al., 2012). Losses of N from soils in the form of N_2O are of particular concern because this greenhouse gas contributes to stratospheric ozone depletion (Portmann et al., 2012; Ramanathan et al., 1985; Ravishankara et al., 2009) and has a 100-year global warming potential that is approximately 300 times that of CO_2 (IPCC, 2014). Moreover, the relationship between N application rate and N_2O emissions from agricultural soils is non-linear (McSwiney and Robertson, 2005; Shcherbak et al., 2014), with N_2O emissions dramatically increasing with moderate increases in fertilization. To mitigate N_2O flux without compromising crop yield, several systems have been developed that include, the maximum return to nitrogen system (Nafziger et al., 2004) and the variable rate nitrogen application system (Scharf et al., 2011). These strategies provide recommendations of fertilization rates that minimize reductions in crop yield while simultaneously decreasing the amount of residual N available for N_2O production, thereby lowering soil N_2O flux. Identifying how to manage the microbial processes contributing to N_2O flux from agricultural systems would be an additional mechanism to mitigate atmospheric N_2O additions (Paustian et al., 2016; Reay et al., 2012; Venterea et al., 2012). Because nitrification and denitrification require aerobic and anaerobic conditions, respectively, strategies directed at controlling soil oxygen saturation could become part of a management strategy (Kravchenko et al., 2017). This, however, requires identifying the relative importance of nitrification and denitrification to N_2O flux spatially and temporally across different agricultural landscapes.

The stable isotope ratios of $\delta^{15}N$ and $\delta^{18}O$ have been used to apportion N_2O flux between nitrification and denitrification (Davidson and Keller, 2000; Park et al., 2011; Yamagishi et al., 2007). Apportionment approaches require that the isotope values of N_2O differ between the two production processes and remain constant throughout the course of a reaction (Jinuntuya-Nortman et al., 2008; Ostrom and Ostrom, 2017). However, shifts or fractionation in the isotope values of N_2O produced during either nitrification or denitrification can compromise source apportionment (Barford et al., 1999; Perez et al., 2000; Sutka et al., 2008; Yoshida, 1988), and reduction of N_2O by denitrification may further alter isotope values (Jinuntuya-Nortman et al., 2008). Nevertheless, $\delta^{15}N$ and $\delta^{18}O$ can still be a useful tool if environmental conditions constrain processes, such as anoxic conditions prohibiting nitrification.

Site preference (SP), the difference in ^{15}N abundance between the central N ($\delta^{15}N^{\alpha}$) and terminal N ($\delta^{15}N^{\beta}$) of N_2O, offers an alternative tool for apportionment of N_2O production (Yoshida and Toyoda, 2000). The large difference in SP of N_2O produced

from nitrification and denitrification (ca. 30 ‰) paired with the observations that SP is constant during N_2O production, and is independent of the isotopic composition of the nitrogen substrates of nitrification and denitrification, has prompted the use of SP for N_2O source apportionment (Sutka et al., 2006; Toyoda et al., 2005). However, SP is not without variation (Toyoda et al., 2017). In addition to production pathway, numerous factors could theoretically control the degree of variation in SP including differences in bacterial species, the specific enzyme involved in its production (Yang et al., 2014), and, for denitrification, carbon source. The accuracy of apportionment estimates using isotope values, including SP, will be improved by understanding sources of variation.

This study investigated the effect of carbon source (electron donor), and carbon source concentration on $\delta^{15}N$ and $\delta^{18}O$ of N_2O produced by two denitrifier species in vitro, as well the effect of these factors on SP values of N_2O. We conducted our study with *Pseudomonas chlororaphis subsp. chlororaphis* and *P. chlororaphis subsp. aureofaciens* because they are highly related denitrifiers that lack N_2O reductase, but encode different nitrite reductases (NIR).

2 Materials and Methods

2.1 Organisms and Culture Conditions

Cultures of *Pseudomonas chlororaphis subsp. chlororaphis* (ATCC 43928; *P. chlororaphis*) and *Pseudomonas chlororaphis subsp. aureofaciens* (ATCC 13985; *P. aureofaciens*) were cryogenically stored (-80 °C) in tryptic soy broth (TSB; Caisson Labs, Smithfield, UT) and sterile glycerol 1:1 (v/v). Stock cultures were re-established in 5 mL TSB amended with sodium nitrate ($NaNO_3$, 10 mM; Sigma-Aldrich, St. Louis, MO) under aerobic conditions at a constant temperature with continuous agitation (18 h, 25 °C). Individual colonies were obtained from re-established stock cultures by the streak-plate technique on tryptic soy agar (TSA; Caisson Labs, Smithfield, UT) amended with $NaNO_3$ (10 mM). Tryptic soy agar plates of stock cultures were sealed with parafilm and incubated (aerobic, 25 °C). The plates were stored at 4 °C for up to two weeks prior to establishment in liquid media for denitrification experiments.

2.2 Preparation of Cultures for Denitrification Experiments

Starter cultures of each species were established in 5 mL TSB amended with $NaNO_3$ (10 mM) with 1 colony from stored stock culture plates (Thermo Fisher Scientific, Waltham, MA). Cultures were then grown aerobically with agitation (25 °C, 18 h) to late exponential phase (optical density at 600 nm (OD_{600}) = 0.3). Optical density was determined with a Spectronic 20 spectrophotometer (Bausch and Lomb, Rochester, NY). Two 160 mL sterile serum bottles containing 50 mL of carbon minimal media (CMM) (Anderson et al., 1993) amended with 10 mM $NaNO_3$ and 10 mM sodium succinate (Sigma-Aldrich, St. Louis, MO) were each inoculated with 200 µL of the aerobic culture. The bottles were stoppered (Geomicrobial Technologies, Inc.), crimp sealed, and the headspace sparged with ultra-high purity (UHP) N_2 for 15 min. Cultures were incubated (25 °C, 18 h) with agitation. Following 18 h, the cells were transferred to 50 mL conical Falcon™ tubes (Corning, Corning, NY) and centrifuged (3,000 x *g*, 30 min, 25 °C) to pellet the cells. The supernatant was decanted and the cells dispersed in CMM lacking

a carbon or nitrogen source (OD_{600} = 0.2). The cells were aliquoted (2 mL) into sterile 35 mL serum bottles, which were then stoppered (Geomicrobial Technologies, Inc.) and crimp sealed. An anaerobic environment was created by sparging the cells with UHP N_2 for 20 min. Sparging was accomplished by inserting one sterile stainless-steel needle (#20 Thomas Scientific, Swedesboro, NJ) carrying N_2 through the stopper into the media while a second sterile stainless-steel needle was inserted through the stopper and into the headspace to allow gas to exit. Following sparging, the bottles were allowed to reach atmospheric pressure, and reactions were then initiated by injecting 20 µL of the carbon source (anaerobic) to reach a final concentration of 0.01 mM, 0.1 mM, 1 mM, or 10 mM. Treatments with citrate and succinate concentrations of 1 mM and 10 mM were conducted for both bacterial taxa. Treatments of citrate and succinate at 0.1 mM were only conducted for *P. chlororaphis*. Treatments with a carbon source concentration of 0.01 mM were only conducted with succinate but were done so for both taxa. The addition of the carbon source was followed by adding 26 µL of 0.1 M $NaNO_3$ (anaerobic) to reach a final NO_3^- concentration of 1.3 mM. The $\delta^{15}N$ and $\delta^{18}O$ of the NO_3^- source was 5.4 ‰ and 24.5 ‰, respectively.

2.3 Isotope Analysis and Modelling Isotope Behaviour

Each treatment consisted of four denitrification cultures. Headspace samples were obtained from each culture with a gas tight syringe (Hamilton; Reno, NV). For one of the four cultures, a 100 µL headspace sample was obtained every 15 minutes for analysis of N_2O concentration. Headspace N_2O concentration of this culture was determined with a Shimadzu Greenhouse Gas Analyzer gas chromatograph equipped with an electron capture detector (ECD) (model GC-2014, Shimadzu Scientific Instruments; Columbio, MD). For details regarding this method see Yang et al. (2014). These data were used to determine when the N_2O concentration was sufficient for isotope analysis and to estimate the volume of headspace required for isotope analysis over the course of the reaction. Headspace sampling of the remaining three cultures was initiated when the N_2O concentration determined by ECD was above ca. 0.4 ppm. Headspace samples between 200 µL and 500 µL of each of the 3 cultures were injected into 60 ml serum bottles (one per culture) that had been sparged with UHP N_2 for 15 min, and stored for isotope analysis. Each bottle contained between 5 nmols and 15 nmols of N_2O for isotopic analysis. Samples were analyzed on an IsoPrime100 stable isotope ratio mass spectrometer (IRMS) interfaced to a TraceGas inlet system (Elementar; Mt. Laurel, NJ) (Sutka et al., 2003). The inlet system used He as the carrier gas and removed both water and CO_2 with separate magnesium perchlorate (Costech; Valencia, CA) and CO_2 absorbent traps (Carbosorb, 8-14 mesh, Costech; Valencia, CA), respectively, prior to concentrating N_2O within a cryofocusing trap. Chromatographic separation of N_2O was achieved with a Porplot Q column prior to isotopic analysis. Mass overlap and related corrections followed the protocol outlined in Toyoda and Yoshida (2000). Our internal laboratory pure N_2O tank standard (MSU Tank B) was isotopically characterized by analysis relative to the USGS51 and USGS52 reference materials (https://isotopes.usgs.gov/lab/referencematerials.html). Following the guidelines proposed by Coplen (2011) we report here the isotope values of the reference materials as well as our internal laboratory standard. The $\delta^{15}N$, $\delta^{18}O$, $\delta^{15}N^{\alpha}$, $\delta^{15}N^{\beta}$, and SP values of USGS51 and USGS52 are 1.3 ‰, 41.2 ‰, 0.5 ‰, 2.2 ‰, and -1.7 ‰ and 0.4 ‰, 40.6 ‰, 13.5 ‰, -12.6 ‰ and 26.2 ‰, respectively. The $\delta^{15}N$, $\delta^{18}O$, $\delta^{15}N^{\alpha}$, $\delta^{15}N^{\beta}$, and SP values of reference MSU Tank C are -0.9 ‰, 0.7 ‰, -2.6 ‰, 39.6 ‰ and 3.4 ‰, respectively. The $\delta^{15}N$, $\delta^{18}O$, $\delta^{15}N^{\alpha}$, $\delta^{15}N^{\beta}$, and SP

values of the isotope standard MSU Tank B are -0.5 ‰, 11.13 ‰, -12.2 ‰, 40.8 ‰ and 23.3 ‰, respectively. All nitrogen isotope values are reported with respect to the international Air-N_2 standard and with respect to VSMOW for $\delta^{18}O$. The mean precision of replicate N_2O standards were 0.1 ± 0.1 ‰, 0.3 ± 0.2 ‰, 0.3± 0.2 ‰, 0.2 ± 0.1 ‰, and 0.6 ± 0.3 ‰ composition for $\delta^{15}N$, $\delta^{15}N^{\alpha}$, $\delta^{15}N^{\beta}$, $\delta^{18}O$, and SP, respectively.

The $\delta^{15}N$ and $\delta^{18}O$ values are reported as:

$$\delta = \left[\left(\frac{R_{sample}}{R_{standard}}\right) - 1\right] \times 1{,}000, \quad (1)$$

where R is the ratio of the trace to the abundant isotope of N or O, and air and VSMOW are the standards for N and O, respectively. Site preference is defined as

$$SP = \delta^{15}N^{\alpha} - \delta^{15}N^{\beta}, \quad (2)$$

where $\delta^{15}N^{\alpha}$ and $\delta^{15}N^{\beta}$ are the isotope values at the central and peripheral N atom of the linear N_2O molecule, respectively. The changes in $\delta^{15}N$, $\delta^{18}O$, and SP of N_2O during the course of the reaction were investigated using the Rayleigh equation by plotting each isotope value vs. [-flnf/(1-f)] where f is the fraction of substrate remaining (Mariotti et al., 1981). According to convention (Mariotti et al., 1981), the magnitude of the isotopic fractionation factor (α) for a single unidirectional reaction is defined by the rate constants of the light (k_1) and heavy (k_2) isotopically substituted compounds:

$$\alpha = k_2/k_1. \quad (3)$$

Further, the isotopic enrichment factor, ε, is defined as

$$\varepsilon = (\alpha - 1) \times 1000, \quad (4)$$

and can be estimated from the slope of the linear relationship described by the Rayleigh model:

$$\delta^{15}N_p = \delta^{15}N_{so} - \varepsilon_{\underline{p}}[(flnf)/(1 - f)]; \quad (5)$$

where $\delta^{15}N_p$ is the isotope value of the accumulated product, $\delta^{15}N_{so}$ is the isotope value of the initial substrate, ε is the fractionation factor, and f is the fraction of substrate remaining (Mariotti et al., 1981). The fraction of substrate remaining was determined by dividing twice the amount of N_2O produced by the total amount of nitrate added, and then subtracting this quantity from 1. Generalized additive modelling of the relationship between the isotope value of N_2O and [-flnf/(1-f)] indicated asymptotic curvilinear behaviour. Therefore, we performed non-linear least squares regression starting with a three-parameter exponential function of the form

$$y = a + ce^{b[x]}. \quad (6)$$

Model reduction and selection were performed following the methods of Baty et al., (2015). Non-linear model fit was also compared to a linear model fit. Models with the lowest residual standard error, fewest iterations to convergence (< 10), lowest parameter confidence intervals, and lowest collinearity of variables were deemed to have the best fit. The goodness of fit for each model was also assessed visually from residual plots. Model residuals that displayed patterns were also deemed poor. This process produced an exponential function with the generalized form

$$y = a + e^{b[x]}, \quad (7)$$

where y is the isotope value of the accumulated product, x is [-flnf/(1-f)], and a and b are coefficients estimated by the model. Values of "a" affect the y-intercept with larger values contributing to increased prediction of the final isotope value of the reaction. Values of "b" affect the rate of change of the isotope values particularly at the beginning of the reaction. Larger values of "b" result in a more gradual rate of change, whereas as lower values of "b" increase the initial slope. The starting values supplied to the function were a = 7 and b = 5 for $\delta^{15}N$ and a = 75 and b =10 for $\delta^{18}O$. These starting values were selected because they are greater than the expected coefficients, which aids in model convergence (Baty et al., 2015). The derivative of Eq. 7,

$$y' = be^{b[x]} \quad (8)$$

can be used to predict the slope at any extent of the reaction. The term net isotope effect (η) has been used to describe isotopic discrimination, the change in isotope value, observed during a multi-step reaction (Jinuntuya-Nortman et al., 2008). Therefore, η is equivalent to y′ in Eq. 8.

We used kernel density estimation to illustrate the density distribution (DD) of η across the extent of the reaction observed. Kernel density estimation is a non-parametric method of determining the probability density function of a random continuous variable. Probability density functions were determined with a Gaussian smoothing kernel from 50 equally spaced estimates of η spanning the complete extent of the reaction (i.e. f = 0 to 1). The bandwidth was set to 1 for each density estimate.

Modelling was performed with R statistical software (Team, 2013), and all figures were produced with ggplot2 (Wickham, 2009, 2011).

2.4 Statistical Analysis of SP Data

We used a linear model to determine if SP changed as a function of [-flnf/(1-f)]. Significant relationships were not observed and therefore the effect of taxa, carbon source, and carbon source concentration on mean SP was examined with Analysis of Variance (ANOVA). Tukey's honest significant difference (HSD) test was used to identify significant differences between and among groups. Normality of the data was assessed with Q-Q plots and the Shapiro-Wilk test.

Statistical analyses were performed with R statistical software (Team, 2013), and all figures were produced with ggplot2 within that software platform (Wickham, 2009, 2011).

3 Results

3.1 Effect of Carbon Source and Concentration on $\delta^{15}N$-N_2O

The $\delta^{15}N$ of N_2O produced by the two denitrifier taxon in our study produced a non-linear relationship with the fraction of substrate remaining expressed in the Rayleigh model as [-flnf/(1-f)] (Figure 1). The derivative, Eq. (5), of the exponential equation for the curvilinear relationship between isotope value and [-flnf/(1-f)] Eq. (4), indicated that $\eta^{15}N$ changed over the course of the reaction (Figure 1, Supplementary Table 1). Estimates of $\eta^{15}N$ during denitrification of NO_3^- to N_2O by *P. aureofaciens* ranged from -77.5 ‰ to -18.4 ‰ and -106.2 ‰ to -11.4 ‰ for citrate and succinate, respectively, while values

ranged from -119 ‰ to -9.2 ‰ and -82.1 ‰ to -5.1 ‰ for citrate and succinate, respectively, during denitrification by *P. chlororaphis* (Figure 2, Supplementary Table 1). Density distributions of $\eta^{15}N$ for all treatments show that the majority of values are of lower magnitude, and values between -50 ‰ and -10 ‰ were most probable. High magnitude values for η occurred at the beginning of reactions, where values of [-flnf/(1-f)] are high (i.e. closer to 1).

3.2 Effect of Carbon Source and Concentration on $\delta^{18}O$-N_2O

The $\delta^{18}O$ of N_2O produced by the two taxa displayed a non-linear relationship with [-flnf/(1-f)] (Figure 1), and much like $\delta^{15}N$, an exponential model Eq. (4) was the most parsimonious fit. The exponential equations determined for each treatment along with the derivatives are presented in Supplementary Documents (Table 2). Similar to the variation in $\eta^{15}N$, the most rapid changes in $\eta^{18}O$ occurred early in the extent of the reactions (i.e. larger values of [-flnf/(1-f)]). Estimates of $\eta^{18}O$ determined following denitrification of NO_3^- by *P. aureofaciens* ranged from -22.2 ‰ to -9.8 ‰ and -77.0 ‰ to -3.1 ‰ for citrate and succinate, respectively, while the reduction of NO_3^- to N_2O by *P. chlororaphis* produced $\eta^{18}O$ values that ranged from -75.4 ‰ to -7.5 ‰ and -67.8 ‰ to -4.0 ‰ for citrate and succinate, respectively. Density distributions of $\eta^{18}O$ indicated that treatments with narrow observed f ranges were not strictly associated with narrow DDs (Figures 1 and 3). For instance, the observed f range for *P. aureofaciens* reduction with 0.01 mM succinate was nearly 0.6 while the range in $\eta^{18}O$ was less than -10 ‰. The rate of change of the function's slope is controlled by parameter b in Eq. (4). Therefore, lower estimates of parameter b produce narrow ranges of $\eta^{18}O$, such as that observed for *P. aureofaciens* reactions with a succinate concentration of 0.01 mM.

3.3 Site Preference as a Function of Carbon-Source and Concentration

Site preference did not change as a function of the extent of the reaction, and across all treatments SP ranged from -7.0 ‰ to 6.0 ‰ (Figure 1). Denitrification by *P. aureofaciens* produced a mean SP of 0 ‰ (st. dev. = 3.3 ‰); however negative SPs observed at 1 mM succinate (mean = -4.2 ‰, st. dev. = 1.8 ‰) contributed greatly to this value (Figure 4). Denitrification of NO_3^- by *P. chlororaphis* produced mean SP values that were similar among all carbon source treatments; -3.7 ‰ (st. dev. = 2.2 ‰) and -4.2 ‰ (st. dev. = 1.2 ‰) for citrate and succinate, respectively.

Analysis of variance identified a significant difference in SP values among the treatments examined for each species (ANOVA, $p < 0.001$). In four of the treatments, the average SP of *P. chlororaphis* denitrification was lower than that of *P. aureofaciens*. This resulted in a difference of 4.1‰ between the average SP of *P. chlororaphis* and *P. aureofaciens*. In addition to taxon, the carbon source (i.e. succinate or citrate) also contributed somewhat to differences in SP between treatments (ANOVA; $p < 0.01$) with growth on succinate producing SP values 0.9 ‰ lower than those produced with citrate as the carbon source. Interestingly, the concentration of the carbon source had no discernible effect on SP under our reaction conditions. Therefore, the variation in SP was largely dependent on taxa (Figure 4).

4 Discussion

This study investigated the effect of denitrifier species, carbon source (electron donor), and electron donor concentration on $\delta^{15}N$, $\delta^{18}O$, and SP isotope values of N_2O produced during denitrification in pure culture. We observed isotopic discrimination against ^{15}N and ^{18}O but no change in SP during the reduction of NO_3^- to N_2O by *P. aureofaciens* or *P. chlororaphis,* and these observations held regardless of carbon source and electron donor concentration.

In contrast to the expectation of the Rayleigh model, the reduction of NO_3^- to N_2O by *P. aureofaciens* and *P. chlororaphis*, displayed a non-linear exponential relationship between $\delta^{15}N$ vs. [-flnf/(1-f)] and $\delta^{18}O$ vs. [-flnf/(1-f)]. This curvilinear isotopic behaviour was evident for denitrification metabolizing both carbon substrates (citrate or succinate) and at all substrate concentrations (Figure 2, Supplementary Table 1). The non-linear behaviour indicates that the fractionation factor, ε, is not constant, a phenomenon not unexpected for multi-step reactions in which more than one enzymatic step and diffusion of products and/or substrates into and out of the cell can result in variation in isotopic discrimination (Granger et al., 2008; Sutka et al., 2008). Because the fractionation factor varies during multi-step reactions, it is best considered a net isotope effect (η) (Jinuntuya-Nortman et al., 2008). The reduction of NO_3^- to N_2O during denitrification involves three enzymes and multiple opportunities for diffusion, all cases where isotope discrimination can occur (Figure 5). Similar to other studies, our previous work on denitrification estimated η from a Rayleigh model (Barford et al., 1999; Lewicka-Szczebak et al., 2014; Sutka et al., 2006; Toyoda et al., 2005; Yano et al., 2014). However, the Rayleigh model assumes a unidirectional single-step reaction with linear behaviour, assumptions that are clearly not valid for N_2O production from nitrate during denitrification. Thus, here we developed estimates of η from the derivative of the exponential relationship between the isotope value of the accumulated product, N_2O, and the extent of the reaction [-f lnf/(1-f)]. This allowed us to quantify changes in η over the course of the denitrification reaction.

For our entire data set, $\eta^{15}N$ and $\eta^{18}O$ varied by as much as ca. 100 ‰ within a single experiment (Figures 2, 3). Note, however, that during N_2O production, both $\delta^{18}O$ and $\eta^{18}O$ can be influenced by oxygen exchange between water and nitrogen oxides (Kool et al., 2009, 2011). These oxygen exchange effects are difficult to quantify making interpretation of $\eta^{18}O$ data difficult. Additionally, visual inspection of the co-variation between $\delta^{18}O$ and $\delta^{15}N$ indicated similar trends among treatments and species, and the observed kinetic isotope effect for $\delta^{18}O$ suggests that there is little exchange with H_2O in the reaction vessels (Figure 1). Thus, we limit our discussion of fractionation to $\eta^{15}N$. Values of $\eta^{15}N$ previously reported for reduction of NO_3^- to N_2O in pure cultures (-43 ‰ to -9 ‰) fall within the range we observed (Sutka et al., 2006; Toyoda et al., 2005; Rohe et al. 2014; Sutka et al 2008). However, some of our values are much greater in magnitude than those previously reported (e.g. -119 ‰). Values of such magnitude occurred near the onset of the reaction (i.e. high values of [-flnf/(1-f)]), most notably when no more than 10 % of the NO_3^- had been reduced. The occurrence of high magnitude η values near the beginning of the reaction is likely related to the relative importance of diffusion and enzymatic fractionation in controlling η. Fractionation associated with enzymes is often much larger than that associated with diffusion, and enzymatic fractionation is fully expressed when diffusion does not limit substrate supply to the enzyme (Jinuntuya-Nortman et al., 2008; Ostrom and Ostrom, 2012). Thus, the

largest η is expected at the beginning of the reaction, consistent with what we observed. Large magnitude values for η can be easily missed if the isotope value of the accumulated product is used to estimate η. Without knowledge of production rate, it can be difficult to know when there is sufficient product for isotopic measurement. By characterizing production rates before initiating experiments to estimate η, we were able to capture isotope values for N_2O close to the onset of the reaction.

There are important reasons why published discrimination factors might be less negative and therefore of lower magnitude than ours. Prior estimates were derived from a single slope from a Rayleigh model and, therefore, do not produce estimates of η over the course of the reaction. Importantly, they may not characterize the large fractionation occurring at the onset of a reaction. Even so, our highly negative values for η might, initially, seem remarkable. Considering variation in η in the context of a multi-step model provides insight into how these values might arise, particularly in the early stages of a culture when the substrate concentration is high. The reduction of NO_3^- to N_2O includes three enzymatic steps in which substantive fractionation may occur (Figure 5). As a consequence, we would expect the products of each successive reaction to become progressively depleted in the heavy isotope, assuming normal ε. If, for example, the ε for each of the three steps was -40 ‰ then reduction of nitrate with a $\delta^{15}N$ of 0 ‰ could yield N_2O of -120 ‰. Thus, denitrification has the potential to produce N_2O that is greatly depleted in ^{15}N resulting in highly negative values for η. As the reaction proceeds, each enzyme is likely to be limited by the supply of substrate from diffusion. This has a tendency to reduce expression of fractionation, and η is therefore reduced to less negative values.

Probability density distributions indicate that markedly low η values associated with one endpoint of the range in η are not common (Figure 3). They also illustrate the range in η that would be expected for the reaction, and their shape emphasizes important changes in η during the course of a reaction. For example, several of the distributions show a marked change in slope on the left side of the distribution (e.g. 10 mM citrate $\eta^{15}N$, both species) that is a consequence of a significant change in slope along the curve of $\delta^{15}N$ vs. [-flnf/(1-f)] (Figures 1, 3). While we cannot ascribe a specific event to this change, future studies aimed at investigating specific enzymes may provide a better understanding of the behaviour of η during denitrification. Perhaps most importantly, these distributions emphasize that assessments of net isotope effects for multi-step reactions will not be complete without consideration of isotopic behaviour over a wide extent of the reaction and the development of models that describe isotope behaviour that does not fit a linear Rayleigh model.

In contrast to the results we observed for $\delta^{15}N$ and $\delta^{18}O$, isotopic discrimination was not evident for SP regardless of treatment (Figure 2). Instead, SP was constant during the course of the reaction. This finding is consistent with pure culture studies of nitrification and denitrification across multiple species (Frame and Casciotti, 2010; Sutka et al., 2003, 2006; Toyoda et al., 2005). The differences we observed in SP between species, however, is likely to relate to the factors that control SP. Unlike the case for bulk isotopes, SP is determined during a single reaction, the reduction of NO to N_2O (Toyoda et al., 2005). Thus, as N_2O reduction does not occur in *P. aureofaciens* or *P. chlororaphis*, SP is only influenced by nitric oxide reductase (NOR) activity and diffusion of NO or N_2O into or out of the cell. As SP is the difference between the $\delta^{15}N$ value of two N atoms that rely on the same NO substrate, SP is not dependent upon the isotopic composition of the initial substrate (Toyoda et al., 2005;

Sutka et al., 2006). The observation that SP remained constant during bacterial denitrification, even though the extent of the reaction varied, (e.g. Sutka et al., 2006) suggests that the expressed fractionation for the α and β N atoms during NO reduction were the same. If so, then one hypothesis is that f can vary markedly and SP will be constant. However, during production of N_2O by pure fungal cytochrome P450 NOR enzyme, distinct fractionation factors for the α and β N atoms were observed and it was proposed that observations of constant SP values during production by fungi were the result of f, or the internal pool size of NO, being held relatively constant during cellular metabolism (Yang et al., 2014). We observed a minor but significant different in SP between two species of *Pseudomonas* sp. during N_2O production that is consistent with a difference in the internal pool size of NO within the cell. The abundance of NO within the cell will depend on its production, reduction, and losses due to diffusion into or out of the cell, all of which could vary between species. We do not know, for example, the degree to which the rate of NO production intrinsically differs between the *cd1*-type NIR of *P. chlororaphis* and copper containing NIR of *P. aureofaciens* or how gene expression may alter these rates. We posit that small differences in SP between and even within species in our study and others may relate to the size of the NO pool available to NOR.

Nitrous oxide is the third most abundant greenhouse gas in the atmosphere and is the greatest source of stratospheric ozone depletion (Ravishankara et al., 2009). Moreover, efforts to balance the N_2O budget have been challenged by the episodic nature of N_2O flux (Nishimura et al., 2005) and, historically, identifying the pathway of N_2O production has been enigmatic (Schreiber et al., 2012). Here we emphasize that within our toolbox, SP remains a robust indicator of N_2O derived from denitrification regardless of carbon source or concentration, and we identify that a component of the variation in SP can be ascribed to species differences. Our ability to understand factors that control variation in SP is important to refining estimates of the relative importance of N_2O production pathways, something that is necessary for mitigation of fluxes of this important GHG from aquatic and terrestrial environments.

Acknowledgments

This work was funded by the DOE Great Lakes Bioenergy Research Center (DOE BER Office of Science DE-FC02-07ER64494). We would like to thank Dr. Hasand Gandhi from Michigan State University for his insight and direction during isotope analyses.

References

Anderson, I. C., Poth, M., Homstead, J. and Burdige, D.: A comparison of NO and N2O production by the autotrophic nitrifier Nitrosomonas europaea and the heterotrophic nitrifier Alcaligenes faecalis, Appl. Environ. Microbiol., 59(11), 3525–3533, 1993.

Barford, C. C., Montoya, J. P. and Altabet, M. A.: Steady-State Nitrogen Isotope Effects of N2 and N2O Production in Paracoccus denitrificans, Appl. Environ. Microbiol., 65(3), 989–994, 1999.

Baty, F., Ritz, C., Charles, S., Brutsche, M., Flandrois, J.-P. and Delignette-Muller, M.-L.: A Toolbox for Nonlinear Regression

in R : The Package nlstools, J. Stat. Softw., 66(5), 1–21, doi:10.18637/jss.v066.i05, 2015.

Coplen, T. B.: Guidelines and recommended terms for expression of stable-isotope-ratio and gas-ratio measurement results, Rapid Commun. Mass Spectrom., 25(17), 2538–2560, doi:10.1002/rcm.5129, 2011.

Davidson, E. A. and Keller, M.: Isotopic variability of N2O emissions from tropical forest soils, Global Biogeochem. Cycles, 14(2), 525–535, 2000.

Denman, K. L.: Climate Change 2007 - The Physical Science Basis: Working Group I Contribution to the Fourth Assessment Report of the IPCC, Cambridge Univ. Press, 499–587 [online] Available from: http://www.amazon.com/Climate-Change-2007-Contribution-Assessment/dp/0521880092, 2007.

Granger, J., Sigman, D. M., Lehmann, M. F. and Tortell, P. D.: Nitrogen and oxygen isotope fractionation during dissimilatory nitrate reduction by denitrifying bacteria, Limnol. Oceanogr., 53(6), 2533–2545, doi:10.4319/lo.2008.53.6.2533, 2008.

IPCC: Summary for Policymakers., 2014.

Jinuntuya-Nortman, M., Sutka, R. L., Ostrom, P. H., Gandhi, H. and Ostrom, N. E.: Isotopologue fractionation during microbial reduction of N2O within soil mesocosms as a function of water-filled pore space, Soil Biol. Biochem., 40, 2273–2280, doi:10.1016/j.soilbio.2008.05.016, 2008.

Kool, D. M., Müller, C., Wrage, N., Oenema, O. and Van Groenigen, J. W.: Oxygen exchange between nitrogen oxides and H2O can occur during nitrifier pathways, Soil Biol. Biochem., 41(8), 1632–1641, doi:10.1016/j.soilbio.2009.05.002, 2009.

Kool, D. M., Wrage, N., Oenema, O., Van Kessel, C. and Van Groenigen, J. W.: Oxygen exchange with water alters the oxygen isotopic signature of nitrate in soil ecosystems, Soil Biol. Biochem., 43(6), 1180–1185, doi:10.1016/j.soilbio.2011.02.006, 2011.

Kravchenko, A. N., Toosi, E. R., Guber, A. K., Ostrom, N. E., Yu, J., Azeem, K., Rivers, M. L. and Robertson, G. P.: Hotspots of soil N2O emission enhanced through water absorption by plant residue, Nat. Geosci., 10(7), 496–500, doi:10.1038/ngeo2963, 2017.

Lewicka-Szczebak, D., Well, R., Köster, J. R., Fuß, R., Senbayram, M., Dittert, K. and Flessa, H.: Experimental determinations of isotopic fractionation factors associated with N2O production and reduction during denitrification in soils, Geochim. Cosmochim. Acta, 134, 55–73, doi:10.1016/j.gca.2014.03.010, 2014.

Mariotti, A., Germon, J. C., Hubert, P., Kaiser, P., Letolle, R., Tardieux, A. and Tardieux, P.: Experimental determination of nitrogen kinetic isotope fractionation: Some principles; illustration for the denitrification and nitrification processes, Plant Soil, 62(3), 413–430, doi:10.1007/BF02374138, 1981.

McSwiney, C. P. and Robertson, G. P.: Nonlinear response of N2O flux to incremental fertilizer addition in a continuous maize (Zea mays L.) cropping system, Glob. Chang. Biol., 11(10), 1712–1719, doi:10.1111/j.1365-2486.2005.01040.x, 2005.

Nafziger, E. D., Sawyer, J. E. and Hoeft, R. G.: Formulating N Recommendations for Corn in the Corn Belt Using Recent Data, Proc. North Cent. Extension-Industry Soil Fertil. Conf., 20, 5–11 [online] Available from: http://www.agronext.iastate.edu/soilfertility/info/nrecNCEISFC-04.pdf, 2004.

Ostrom, N. E. and Ostrom, P. H.: Handbook of Environmental Isotope Geochemistry, edited by M. Baskaran, pp. 453–476,

Springer-Verlag, Heidelberg., 2012.

Ostrom, N. E. and Ostrom, P. H.: Mining the isotopic complexity of nitrous oxide: a review of challenges and opportunities, Biogeochemistry, 132(3), 359–372, doi:10.1007/s10533-017-0301-5, 2017.

Pan, B., Lam, S. K., Mosier, A., Luo, Y. and Chen, D.: Ammonia volatilization from synthetic fertilizers and its mitigation strategies: A global synthesis, Agric. Ecosyst. Environ., 232, 283–289, doi:10.1016/j.agee.2016.08.019, 2016.

Park, S., Pérez, T., Boering, K. A., Trumbore, S. E., Gil, J., Marquina, S. and Tyler, S. C.: Can N2O stable isotopes and isotopomers be useful tools to characterize sources and microbial pathways of N2O production and consumption in tropical soils?, Global Biogeochem. Cycles, 25(1), doi:10.1029/2009GB003615, 2011.

Paustian, K., Lehmann, J., Ogle, S., Reay, D., Robertson, G. P. and Smith, P.: Climate-smart soils, Nature, 532(7597), 49–57, doi:10.1038/nature17174, 2016.

Perez, T., Trumbore, S. E., Tyler, S. C., Davidson, E. A., Keller, M. and de Camargo, P. B.: Isotopic variability of N2O emissions from tropical forest soils, Global Biogeochem. Cycles, 14(2), 525–535, 2000.

Portmann, R. W., Daniel, J. S. and Ravishankara, A. R.: Stratospheric ozone depletion due to nitrous oxide: influences of other gases, Philos. Trans. R. Soc. B Biol. Sci., 367(1593), 1256–1264, doi:10.1098/rstb.2011.0377, 2012.

Ramanathan, V., Cicerone, R. J., Singh, H. B. and Kiehl, J. T.: Trace gas trends and their potential role in climate change, J. Geophys. Res., 90(D3), 5547–5566, doi:10.1029/JD090iD03p05547., 1985.

Ravishankara, A. R., Daniel, J. S. and Portmann, R. W.: Nitrous oxide (N2O): the dominant ozone-depleting substance emitted in the 21st century., Science (80-.)., 326(5949), 123–125, doi:10.1126/science.1176985, 2009.

Reay, D. S., Davidson, E. A., Smith, K. A., Smith, P., Melillo, J. M., Dentener, F. and Crutzen, P. J.: Global agriculture and nitrous oxide emissions, Nat. Clim. Chang., 2(6), 410–416, doi:10.1038/nclimate1458, 2012.

Robertson, G. P. and Vitousek, P. M.: Nitrogen in Agriculture: Balancing the Cost of an Essential Resource, Annu. Rev. Environ. Resour., 34(1), 97–125, doi:10.1146/annurev.environ.032108.105046, 2009.

Scharf, P. C., Shannon, D. K., Palm, H. L., Sudduth, K. A., Drummond, S. T., Kitchen, N. R., Mueller, L. J., Hubbard, V. C. and Oliveira, L. F.: Sensor-based nitrogen applications out-performed producer-chosen rates for corn in on-farm demonstrations, Agron. J., 103(6), 1683–1691, doi:10.2134/agronj2011.0164, 2011.

Schreiber, F., Wunderlin, P., Udert, K. M. and Wells, G. F.: Nitric oxide and nitrous oxide turnover in natural and engineered microbial communities: Biological pathways, chemical reactions, and novel technologies, Front. Microbiol., 3(October), 1–24, doi:10.3389/fmicb.2012.00372, 2012.

Sebilo, M., Mayer, B., Nicolardot, B., Pinay, G. and Mariotti, A.: Long-term fate of nitrate fertilizer in agricultural soils, Proc. Natl. Acad. Sci., 110(45), 18185–18189, doi:10.1073/pnas.1305372110, 2013.

Shcherbak, I., Millar, N. and Robertson, G. P.: Global metaanalysis of the nonlinear response of soil nitrous oxide (N2O) emissions to fertilizer nitrogen, Proc. Natl. Acad. Sci., 111(25), 9199–9204, doi:10.1073/pnas.1322434111, 2014.

Sutka, R. L., Ostrom, N. E., Ostrom, P. H., Gandhi, H. and Breznak, J. A.: Nitrogen isotopomer site preference of N2O produced by Nitrosomonas europaea and Methylococcus capsulatus bath, Rapid Commun. Mass Spectrom., 17(7), 738–745,

doi:10.1002/rcm.968, 2003.

Sutka, R. L., Ostrom, N. E., Ostrom, P. H., Breznak, J. A., Pitt, A. J., Li, F. and Gandhi, H.: Distinguishing Nitrous Oxide Production from Nitrification and Denitrification on the Basis of Isotopomer Abundances, Appl. Environ. Microbiol., 72(1), 638–644, doi:10.1128/AEM.72.1.638, 2006.

Sutka, R. L., Adams, G. C., Ostrom, N. E. and Ostrom, P. H.: Isotopologue fractionation during N2O production by fungal denitrification, Rapid Commun. Mass Spectrom., 22(24), 3989–3996, doi:10.1002/rcm.3820, 2008.

Team, R.: R Development Core Team, R A Lang. Environ. Stat. Comput., 55, 275–286 [online] Available from: http://www.mendeley.com/research/r-language-environment-statistical-computing-96/%5Cnpapers2://publication/uuid/A1207DAB-22D3-4A04-82FB-D4DD5AD57C28, 2013.

Toyoda, S., Mutobe, H., Yamagishi, H., Yoshida, N. and Tanji, Y.: Fractionation of N2O isotopomers during production by denitrifier, Soil Biol. Biochem., 37(8), 1535–1545, doi:10.1016/j.soilbio.2005.01.009, 2005.

Toyoda, S., Yoshida, N. and Koba, K.: Isotopocule analysis of biologically produced nitrous oxide in various environments, Mass Spectrom. Rev., 36, 135–160, doi:10.1002/mas, 2017.

Venterea, R. T., Halvorson, A. D., Kitchen, N., Liebig, M. A., Cavigelli, M. A., Del Grosso, S. J., Motavalli, P. P., Nelson, K. A., Spokas, K. A., Singh, B. P., Stewart, C. E., Ranaivoson, A., Strock, J. and Collins, H.: Challenges and opportunities for mitigating nitrous oxide emissions from fertilized cropping systems, Front. Ecol. Environ., 10(10), 562–570, doi:10.1890/120062, 2012.

Wickham, H.: ggplot2. [online] Available from: http://books.google.com/books?id=rhRqtQAACAAJ&dq=intitle:ggplot2+inauthor:wickham&ie=ISO-8859-1&source=gbs_gdata, 2009.

Wickham, H.: ggplot2, Wiley Interdiscip. Rev. Comput. Stat., 3(2), 180–185, doi:10.1002/wics.147, 2011.

Yamagishi, H., Westley, M. B., Popp, B. N., Toyoda, S., Yoshida, N., Watanabe, S., Koba, K. and Yamanaka, Y.: Role of nitrification and denitrification on the nitrous oxide cycle in the eastern tropical North Pacific and Gulf of California, J. Geophys. Res. Biogeosciences, 112(2), 1–15, doi:10.1029/2006JG000227, 2007.

Yang, H., Gandhi, H., Ostrom, N. E. and Hegg, E. L.: Isotopic Fractionation by a Fungal P450 Nitric Oxide Reductase during the Production of N 2 O, Environ. Sci. Technol., 48(18), 10707–10715, doi:10.1021/es501912d, 2014.

Yano, M., Toyoda, S., Tokida, T. and Hayashi, K.: Soil Biology & Biochemistry Isotopomer analysis of production , consumption and soil-to- atmosphere emission processes of N 2 O at the beginning of paddy fi eld irrigation, Soil Biol. Biochem., 70, 66–78, doi:10.1016/j.soilbio.2013.11.026, 2014.

Yoshida, N.: 15N-depleted N2O as a product of nitrification, Nature, 335, 528–529, doi:10.1038/335528a0, 1988.

Yoshida, N. and Toyoda, S.: Constraining the atmospheric N2O budget from intramolecular site preference in N2O isotopomers, Nature, 405(6784), 330–4, doi:10.1038/35012558, 2000.

Zhou, M. and Butterbach-Bahl, K.: Assessment of nitrate leaching loss on a yield-scaled basis from maize and wheat cropping systems, Plant Soil, 374(1–2), 977–991, doi:10.1007/s11104-013-1876-9, 2014.

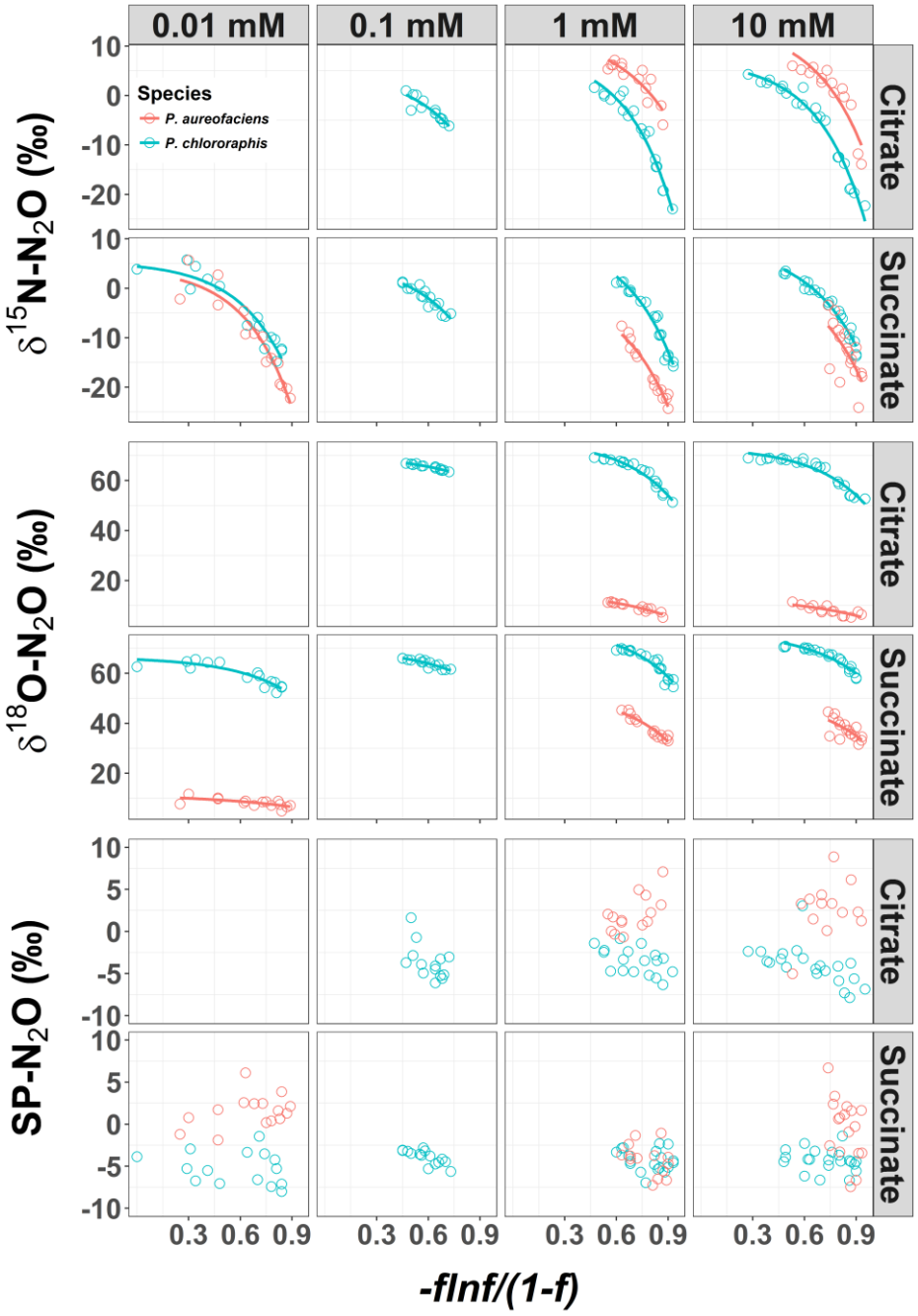

Figure 1: $\delta^{15}N$, $\delta^{18}O$, and site preference (SP) of N_2O produced during denitrification of NO_3^- by *Pseudomonas chlororaphis subsp. aureofaciens* and *Pseudomonas chlororaphis subsp. chlororaphis* with different electron donor sources and concentrations. A larger value of [-flnf/(1-f)], where f is the fraction of substrate remaining, represents earlier points in the reaction. The curved relationships are of the form $y = a + e^{b[x]}$, where y is the isotope value, x is [-flnf/(1-f)] and a and b are the estimated coefficients that affect the y-intercept and curvilinear shape, respectively.

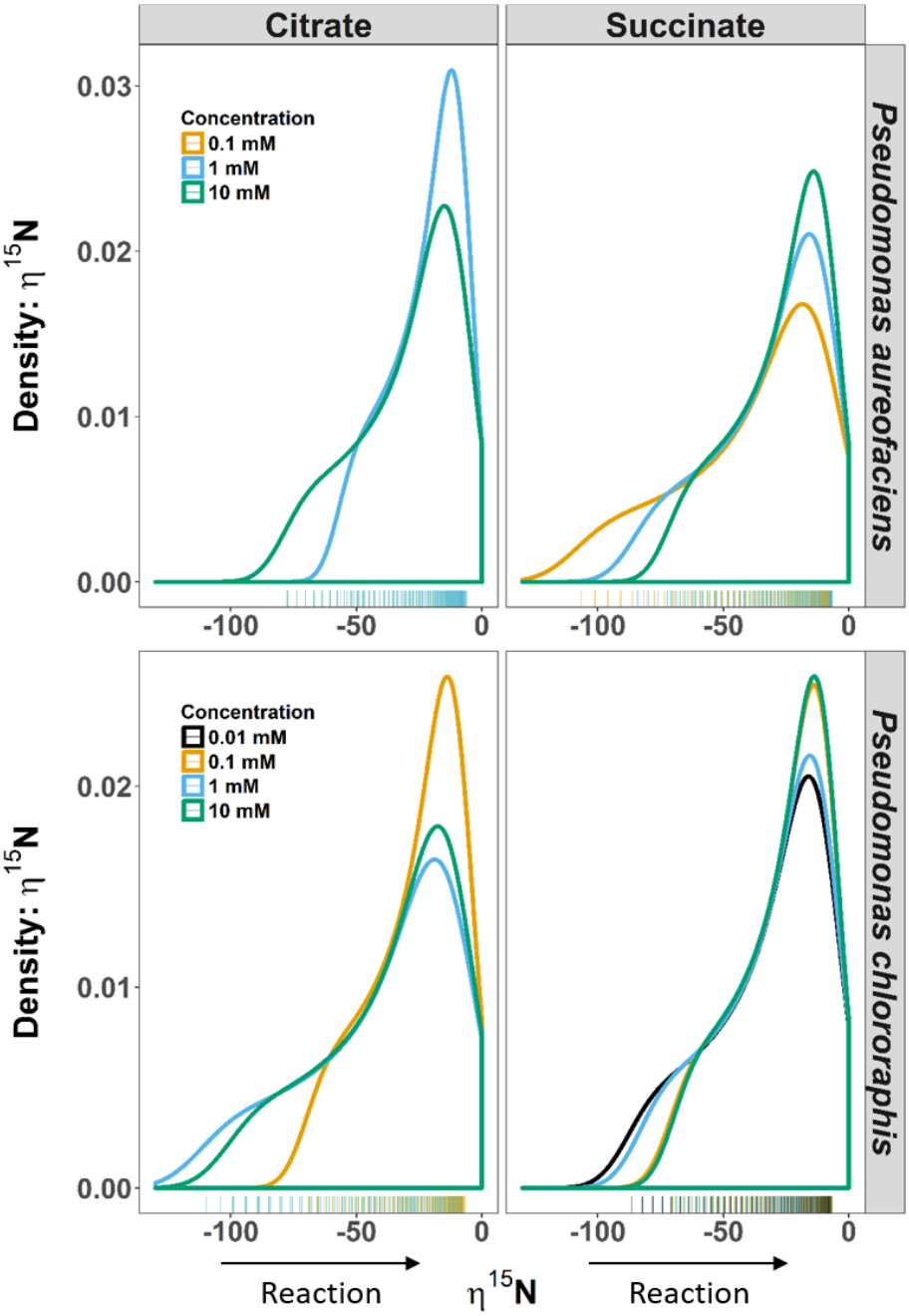

Figure 2. Density distributions (DD) of $\delta^{15}N$ net isotope effects (η) derived from the derivative of the exponential function (Eq. 4) describing the relationship between $\delta^{15}N$ and [-flnf/(1-f)] for *Pseudomonas aureofaciens* (orange) and *Pseudomonas chlororaphis* (blue). Estimates of η were produced over the entire extent of the reaction (i.e. f=0 to 1). The left panel displays the PDDs for citrate treatments and the right for succinate treatments. Positive values of η were not observed during reactions. Tally marks at the base of each panel indicate the actual distribution of calculated values.

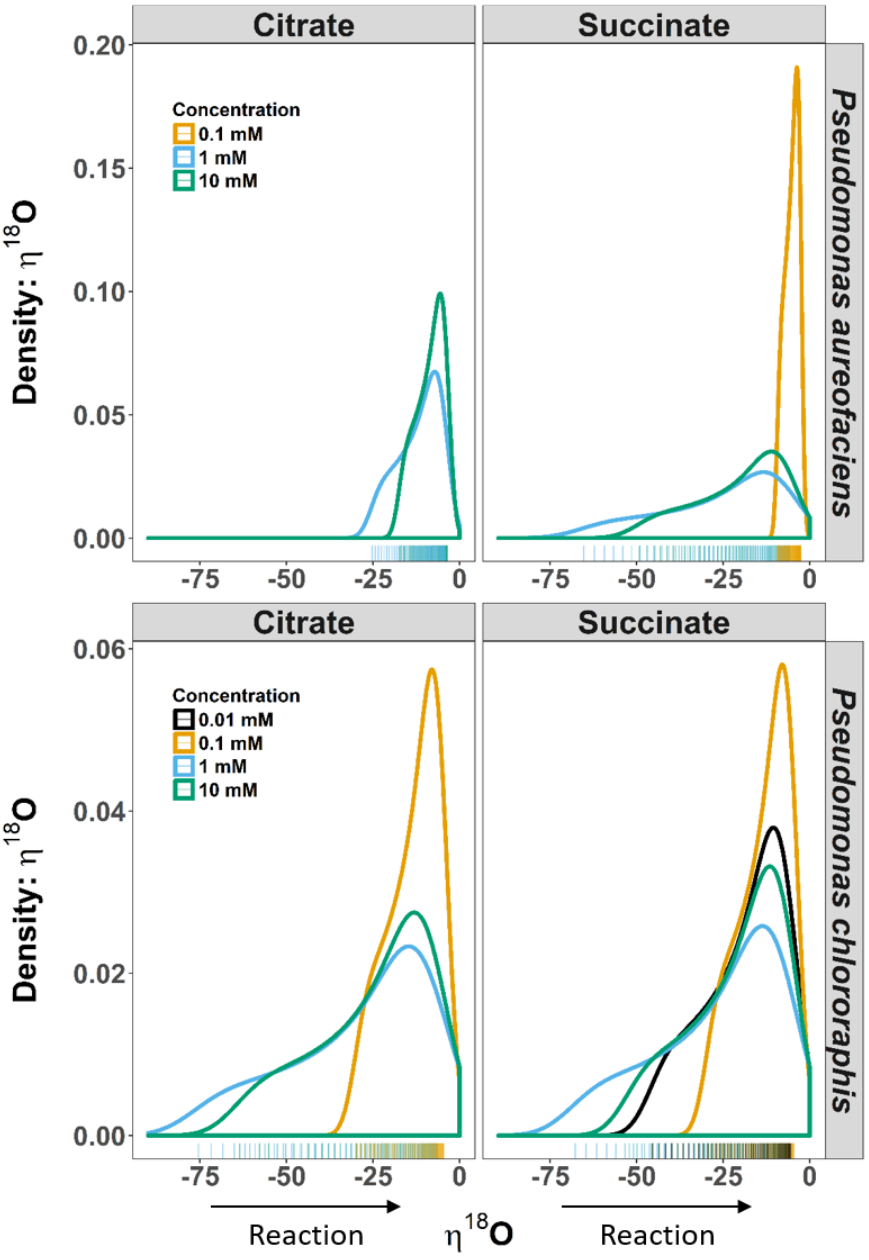

Figure 3. Density distributions (DD) of $\delta^{18}O$ net isotope effects (η) estimated from the derivative of an exponential function describing the relationship between $\delta^{18}O$ and [-flnf/(1-f)] for *Pseudomonas aureofaciens* (orange) and *Pseudomonas chlororaphis* (blue). The estimates of η are extrapolated to include the complete extent of the reaction. The left panel displays the PDDs for citrate treatments and the right for succinate treatments. Positive values of η were not observed during reactions. Tally marks at the base of each panel indicate the actual distribution of calculated values.

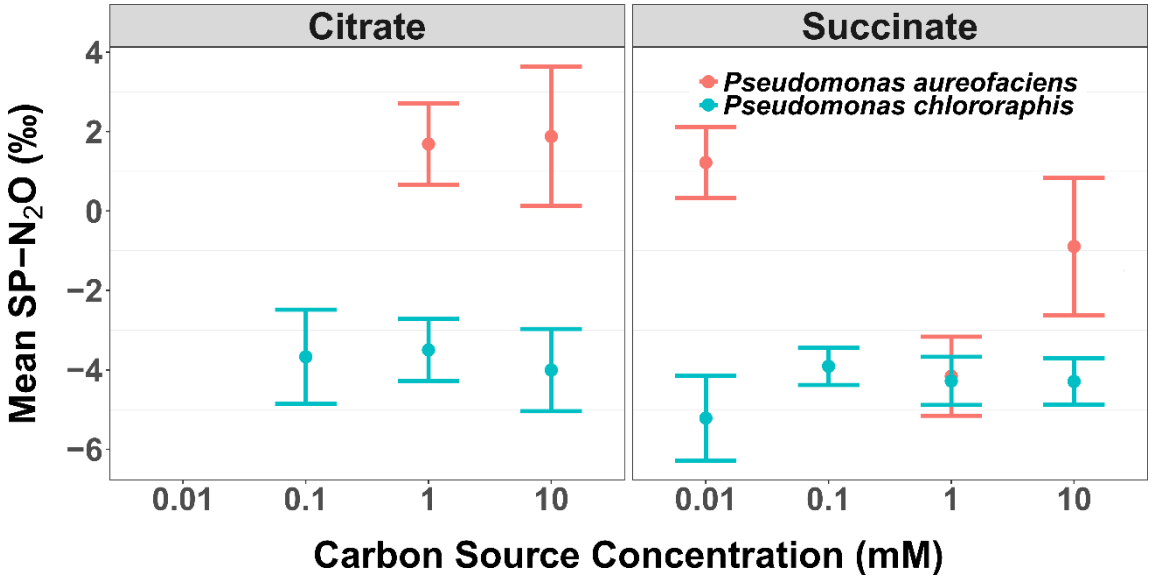

Figure 4. The mean site preference (SP) of N_2O produced during the reduction of NO_3^- by *Pseudomonas aureofaciens* (orange) and *Pseudomonas chlororaphis* (blue) with different concentrations of electron donors: citrate and succinate. Error bars indicate 1 standard deviation.

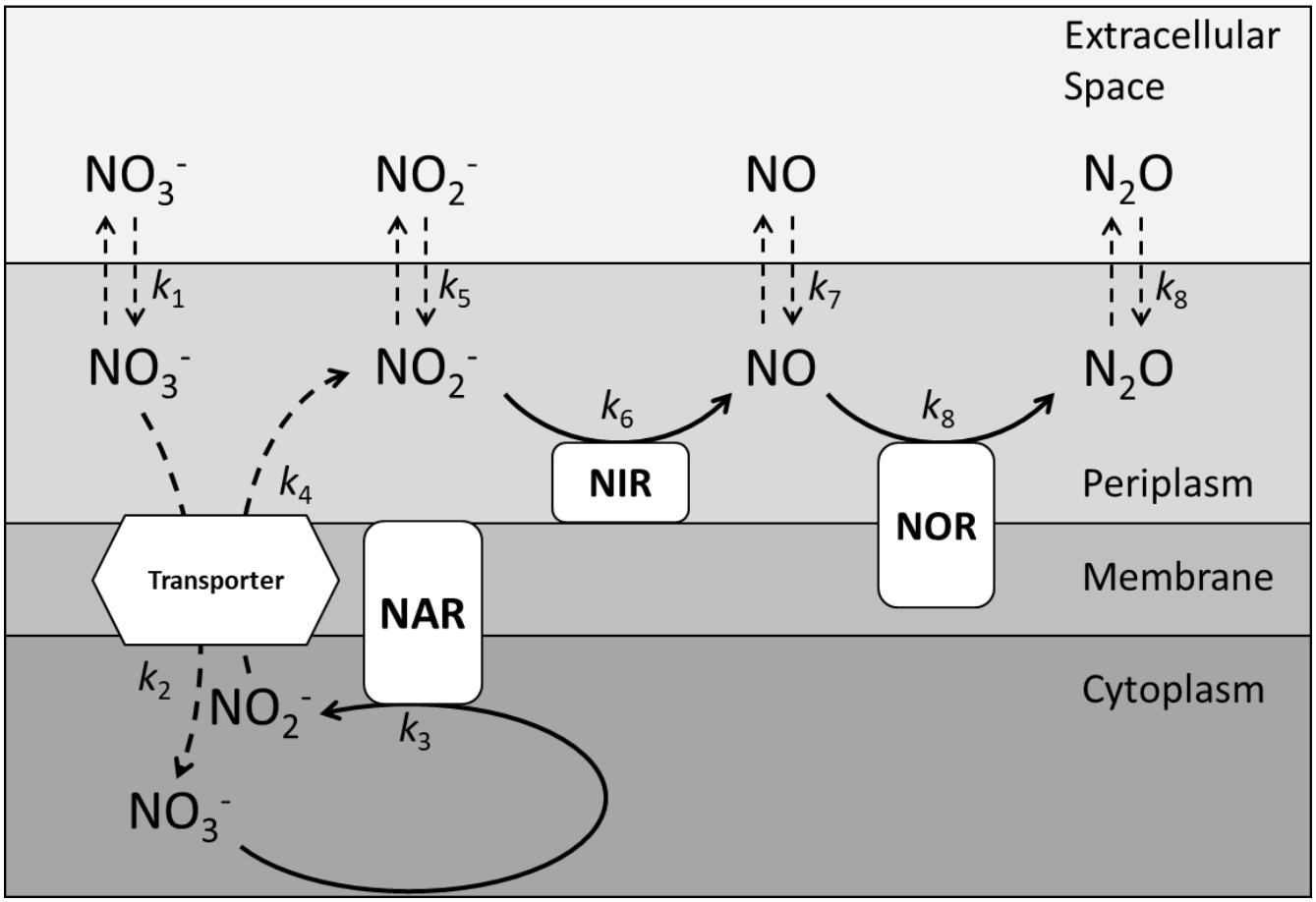

Figure 5. A schematic representation of the multi-step reduction of nitrate to nitrous oxide during denitrification specific to *Pseudomonas aureofaciens* and *Pseudomonas chlororaphis*, which lack the enzyme nitrous oxide reductase. The enzymes responsible for the reduction of nitrogen species appear in boxes with rounded corners and are indicated by three letter sequences: nitrate reductase (NAR), nitrite reductase (NIR), and nitric oxide reductase (NOR). A nitrate/nitrite transporter protein is presented as a hexagon. The position of the enzymes with respect to the periplasm, membrane, or cytoplasm identify the location of the enzymes in the cell. Vertical dashed arrows indicate diffusion of various nitrogen species into and out of the cell, and curved dashed arrows represent transport across the membrane. Solid arrows represent enzyme catalysed reduction steps.